Jurnal Polimesin
Department of Mechanical Engineering
State Polytechnic of Lhokseumawe
http://e-jurnal.pnl.ac.id/polimesin
e-ISSN : 2549-1999 No. : 3 Month : June
p-ISSN : 1693-5462 Volume : 24 Year : 2026

Processing dates: received on 2026-03-30, reviewed on 2026-05-25, accepted on 2026-06-07 and online availability on 2026-06-30

Influence of machining parameters on cutting performance and wear mechanisms of coated carbide tools

Fransnazoan Sitorus[1,*], Naqasya Asyrori Sidabutar[1], Sumawijaya Suyatno[2], Ulfani Ikhwana Purba[3], Derlini[3]
[1]Department of Mechanical Engineering, Politeknik Teknologi Kimia Industri, Medan 20228, Indonesia
[2]Department of Mechanical Engineering, Faculty of Science and Technology, Universitas Samudra, Langsa 24416, Indonesia
[3]Department of Mechanical Engineering, Universitas Pembinaan Masyarakat Indonesia, Medan 20217, Indonesia
*Corresponding Author: fransnazoanstr@gmail.com

Abstract

In coated carbide cutting tools, the coating layer functions as a solid lubricant that improves wear resistance and minimizes frictional and thermal effects during machining. This study investigates the influence of machining parameters on cutting performance and characterizes the coating material and WC/Co carbide substrate to better understand their relationship with tool wear behavior. The machining parameters were established through an experimental design that evaluated mechanical loading, thermal loading, and chemical interactions using microstructural analysis. The experimental design evaluated the effects of mechanical loading, thermal loading, and chemical interactions through wear and microstructural analysis. Under mechanical loading, machining of Al-6061 produced mild abrasive wear with flank wear (VB) of 0.07 mm, while AISI 1070 generated higher edge wear of 0.25 mm. Under thermal loading, a 20% increase in cutting speed resulted in VB of 0.10 mm for Al-6061, whereas a 20% reduction in cutting speed for AISI 1070 produced VB of 0.16 mm accompanied by plastic deformation. Chemical interaction analysis showed stable coating integrity without delamination during Al-6061 machining. In contrast, AISI 1070 machining caused partial diamond film loss and substrate exposure, with approximately 35% diamond film remaining after wear progression. The results indicate that tool wear behavior is mainly controlled by mechanical loading, while thermal and chemical effects remain secondary. Abrasive wear was identified as the dominant wear mechanism, causing progressive coating removal without catastrophic delamination.

Keywords:
Machining parameters; coated carbide tools; mechanical and thermal loading; chemical interaction; coating wear mechanism

1 Introduction

Research on machining processes continues to expand to improve productivity, efficiency, and overall machining performance. A key technological advancement has been the development of tool coating systems, which have proven effective in enhancing machining productivity and prolonging tool life. Consequently, numerous advanced coating materials and architectures have been developed to address the growing demands and complexity of modern machining applications [1][2].

In coating technology, coating materials act as solid lubricants that play an important role in minimizing friction and thermal during the cutting process [3]. However, achieving a more comprehensive understanding of the performance characteristics of coated carbide tools remains challenging and warrants further investigation. It is widely used in the metal cutting industry, particularly for aluminum-based component manufacturing remains necessary. Accordingly, further investigations are required to elucidate the relationships between coating characteristics, cutting performance, and tool wear behavior under various machining conditions. Based on previous analyses, three key parameters must be considered to minimize tool wear, namely cutting speed, tool nose radius, and rake angle [4]. These parameters play a crucial role in governing the wear behavior and service life of coated carbide cutting tools and therefore must be carefully selected and optimized in machining applications.

Previous studies have reported that TiAlN/Al_2O_3- and TiN-coated carbide tools failed during the machining of hard-faced camshaft materials, as evidenced by flank wear, crater wear, coating delamination, and Built-Up Edge (BUE) formation [5]. In addition, study [6] experimentally investigated the machining of ASTM A29 steel using TiAlN-coated carbide tools and demonstrated that acceptable cutting performance can be achieved under specific machining parameters and conditions. Conversely, study [7] reported that coated carbide tools did not perform optimally during the machining of non-ferrous materials. This study identified coating delamination as the dominant wear phenomenon, characterized by the separation of the coating layer from the carbide substrate during cutting. Coating peeling was also observed at the early stage of machining, particularly during the initial wear period. These results indicate that coating failure mechanisms are strongly dependent on workpiece material properties and cutting conditions. Therefore, further research is required to enhance the understanding of wear behavior and coating durability under a wide range of machining conditions.

Various machining conditions have been investigated, including dry machining and the use of cooling media under minimum quantity lubrication (MQL) conditions. A study conducted by [8] examined the performance and wear mechanisms of PVD TiAlN-NbN-coated cemented carbide tools during the milling of Ti6Al4V under different lubrication strategies. The results indicated that tool life under dry machining and MQL conditions was relatively similar. The wear behavior was mainly dominated by mechanical fracture mechanisms, which significantly contributed to tool degradation. In addition, the wear process was intensified by carbon diffusion from the WC substrate and Co-binder. Oxidation of the Co binder further reduced the mechanical strength of the tool material. These findings suggest that mechanical fracture is the primary wear mechanism controlling tool degradation, while elemental diffusion and binder oxidation act as secondary factors that accelerate wear progression during the machining of Ti6Al4V titanium alloy.

Research on the evolution of flank and rake face wear in PVD-coated carbide cutting tools during turning operations has been reported by [9]. The study demonstrated that the fatigue critical strain decreases markedly with increasing strain rate, which consequently leads to a significant reduction in tool life. As stated in [9], higher strain rates restrict the time available for dislocation movement within the material, resulting in the formation of localized high-stress regions. This condition reduces material ductility, increases brittleness, and lowers the fatigue critical strain. These results indicate that coating fatigue is the dominant wear mechanism governing tool degradation. Accordingly, tool life can be predicted by accounting for the influence of strain rate on fatigue behavior and the associated coating degradation mechanisms.

The performance of Nanocrystalline Diamond (NCD) coated cutting tools was investigated during the machining of aluminum alloys. For comparative analysis, conventional Chemical Vapor Deposition (CVD) Microcrystalline Diamond (MCD) coated tools and Polycrystalline Diamond (PCD) tools were also evaluated under similar machining conditions [10]. The results revealed that cutting speed plays a dominant role in the failure behavior of coated carbide tools. In dry turning of non-ferrous materials using NCD-coated

carbide tools, coating failure was primarily governed by the applied cutting speed. These findings indicate that cutting speed is a critical machining parameter influencing the durability and wear resistance of NCD-coated carbide tools during the machining of aluminum alloys.

A study reported by [11] investigated the wear mechanisms of Al_2O_3-coated carbide tools during the turning of mild steel. Machining operations conducted at cutting speeds ranging from 100 to 600 m/min revealed that the Al_2O_3 coating underwent rapid and localized degradation. The findings also revealed chemical interactions between the alumina coating and non-metallic inclusions in the workpiece material. Experimental measurements using infrared thermography revealed cutting temperatures ranging from 850 to 1000°C. Furthermore, the study demonstrated that coating degradation during the steel turning process was primarily governed by chemical reactions between the alumina coating and Ca- and Mg-based non-metallic inclusions.

To investigate and predict the chemical degradation mechanisms of aluminum oxide-coated cutting tools, a study was carried out using high-pressure diffusion couples, advanced microscopy techniques, and thermodynamic analyses [12]. The study examined the interactions between the aluminum oxide coating, steel, and various combinations of non-metallic inclusions. The results showed that alumina possesses high resistance to chemical degradation when interacting with steel under oxygen-free conditions. However, this resistance decreases in the simultaneous presence of ambient oxygen and non-metallic inclusions within the cutting environment. The integration of experimental data, advanced microscopic observations, and thermodynamic modeling provided a comprehensive understanding of the chemical degradation behavior of alumina-coated tools during machining processes. These findings indicate that chemical interactions between the coating layer, non-metallic inclusions, and the cutting environment play a critical role in governing coating degradation mechanisms.

The wear mechanisms of PVD (Ti, Al) N-coated carbide tools and their chemical interactions with 316L stainless steel during turning operations were investigated by [13]. The results showed that excessively high contact pressure suppresses the formation of protective deposits at the tool edge, whereas excessively low contact pressure may also result in accelerated wear. Therefore, a specific operating window is required to promote the preferential deposition of two identified protective non-metallic inclusions, namely $Mg_1Al_2O_4$ and $Al_2Ca_2Si_1O_7$, on the tool surface. Furthermore, [13] experimentally clarified the underlying wear mechanisms and demonstrated that the effectiveness of coating protection is not solely determined by the presence of non-metallic inclusions, but is also strongly influenced by contact conditions that enable the formation of stable protective deposits during turning operations.

The investigation of tool wear is crucial for understanding the effects of machining parameters on coating delamination. A study conducted by [14] evaluated nano diamond-coated cutting tools during the machining of aluminum matrix composites. The results indicated that tool wear evolution consisted of an initial stage characterized by a low wear rate, followed by a rapid increase in flank wear associated with coating delamination. This wear pattern was consistently observed across all machining conditions investigated. Moreover, the feed rate was identified as the dominant parameter influencing the cutting duration before coating delamination, primarily due to increased mechanical loading. The study further demonstrated that nano diamond-coated tools exhibit higher resistance to delamination compared with conventional MCD-coated tools.

Coating delamination represents a critical tool wear mechanism that can be initiated by mechanical loading, thermal loading, or chemical interactions between the workpiece material and the cutting tool. During this process, the coating layer separates from the tool substrate when cutting forces, elevated temperatures, or chemical reactions exceed the interfacial adhesion strength. Once delamination occurs, the coating can no longer effectively serve its protective function. Consequently, the expected advantages of tool coatings, including improved wear resistance, enhanced tool performance, increased productivity, and the ability to operate at higher cutting speeds, cannot be fully realized. Thus, the performance benefits associated with coated tools are significantly compromised when coating integrity is lost.

This study investigates the influence of machining parameters on cutting performance, with particular emphasis on the characterization of coating materials and carbide tool substrates related to wear mechanisms arising from the combined effects of mechanical loading, thermal loading, and chemical interactions between the workpiece material and the cutting tool under dry machining conditions. Special attention is given to diamond film coatings and WC/Co carbide substrates. This study aims to improve the understanding of the wear behavior of diamond film-coated carbide tools under various machining parameters.

The findings of this study are expected to provide a more comprehensive understanding of the influence of machining parameters on coating wear mechanisms and to support efforts to enhance the performance of diamond film-coated carbide tools in metal cutting applications. In particular, the results are anticipated to offer valuable insights for the planning and optimization of machining processes in relation to cutting performance and the wear characteristics of diamond film-coated carbide tools used as protective coatings on cutting tools. Furthermore, the outcomes of this study are expected to contribute to the development of more effective strategies for improving tool life, wear resistance, and machining performance under dry machining conditions.

2 Research methodology

2.1 Terminology of the turning process

In a turning operation, the workpiece is mounted in a chuck and rotated about its longitudinal axis, whereas the cutting tool moves linearly to remove material from the workpiece surface. Metal cutting is a complex process characterized by the simultaneous interaction of mechanical, thermal, and tribological effects [15]. The principal machining parameters influencing the turning process are spindle speed (n), feed rate (f), and depth of cut (a), as illustrated in Fig. 1.

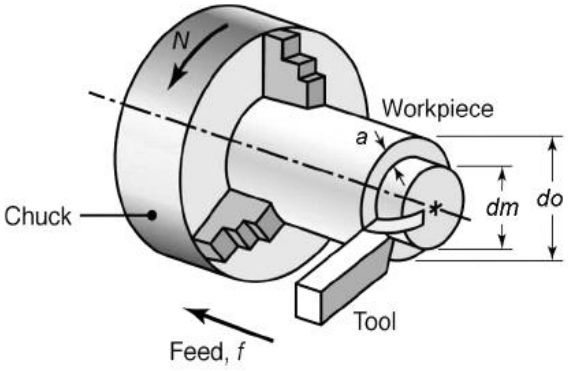

Fig. 1. Schematic illustration of the turning process

The machining process consists of five fundamental elements, as reported in [16], namely: 1. Cutting speed (v, m/min) 2. Feed rate (vf, mm/min); 3. Depth of cut (a, mm); 4. Cutting time (tc, min); and 5. Material removal rate (Z, cm³/min). To establish the cutting conditions, the equations governing the principal turning parameters are employed, as reported in [15].

a. Cutting speed (Eq. (1)), where v denotes the cutting speed (m/min), d represents the average workpiece diameter (mm), and n is the spindle speed (rpm).

$$v = \frac{\pi . d . n}{1000} \quad (1)$$

b. Feeding rate (Eq. (2)), where f denotes the feed per revolution (mm/rev).

$$f = \frac{mm}{rev} \tag{2}$$

c. Feeding speed (Eq. (3)), where vf denotes the feed speed (mm/min), f represents the feed rate (mm/rev), and n is the spindle speed (rpm).

$$vf = f.n \tag{3}$$

d. Depth of cut (Eq. (4)), where a denotes the depth of cut (mm), d_o represents the initial diameter (mm), and d_m is the final diameter (mm).

$$a = \frac{d_o - d_m}{2} \tag{4}$$

e. Cutting time (Eq. (5)), where tc denotes the cutting time (min), lt represents the machining length (mm), and vf is the feed speed (mm/min).

$$tc = \frac{lt}{Vf} \tag{5}$$

f. Machining length (Eq. (6)), where lt denotes the total machining length (mm), l represents the actual machining length (mm), la is the tool approach allowance (mm), and lo is the tool overtravel allowance (mm).

$$lt = l + la + lo \tag{6}$$

2.2 Failure characteristics of cutting tools

The effect of tool failure on machining performance is manifested through decreased dimensional accuracy, increased surface roughness, higher cutting temperatures, increased cutting forces, intensified vibration, decreased production efficiency, and increased manufacturing costs. The characteristics and underlying mechanism of tool failure may contribute to premature termination of tool life. Fig. 2 illustrates the various modes of tool failure.

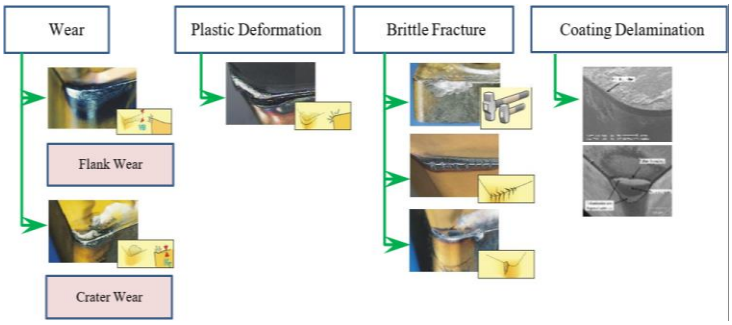

Fig. 2. Classification of tool failure mode

2.3 Material testing

This study employed Aluminium Al-6061 AlMgSiCu as the test material, in the form of a cylindrical workpiece with a length of 220 mm and a diameter of 145 mm. The material was selected for its excellent machinability and widespread use in aerospace components, marine structures, pistons, brake pistons, and other engineering applications [17]. The chemical composition, hardness values, and workpiece geometry are presented in Table 1, Table 2, and Fig. 3, respectively.

Table 1. Chemical composition of Al-6061 AlMgSiCu

Element	Al	Si	Fe	Cu	Mn	Mg	Zn	Cr	Ni	Ti	Ca	Pb	Sn	V	Bi	Zr	Ga	Co	Hg	In	Sb	La
wt.	98.1	0.577	0.001	0.163	0.034	0.929	0.050	0.089	0.002	0.011	0.004	0.001	0.002	0.009	0.003	0.001	0.007	0.002	0.002	0.003	0.010	0.001

Table 2. Hardness value of Al-6061 AlMgSiCu

Material testing	I	II	III	HRB
Al-6061	53	53.5	53	53.2

AISI 1070 was prepared in the form of a cylindrical bar with an effective length of 210 mm and a diameter of 65 mm. The chemical composition, hardness values, and workpiece geometry are presented in Table 3, Table 4, and Fig. 4, respectively

Table 3. Chemical composition of AISI 1070

Element	Fe	C	Si	Mn	p	s	Cr	Mo	Ni	Al	Cu	Co	Ti	Nb	w	v
wt. [%]	97.8	0.796	0.258	0.790	0.025	0.011	0.151	0.089	0.008	0.039	0.004	0.001	0.005	0.005	0.015	0.005

Table 4. Rockwell hardness of AISI 1070 steel

Material Testing	I	II	III	HRB
AISI 1070	93.5	93	93.5	93.8

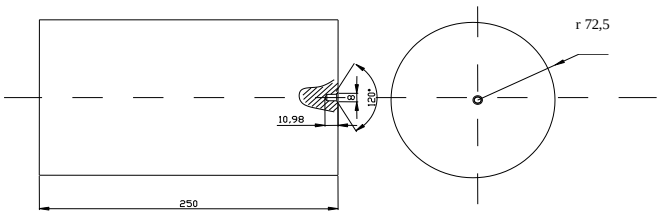

Fig. 3. Aluminium Al-6061 AlMgSiCu test material

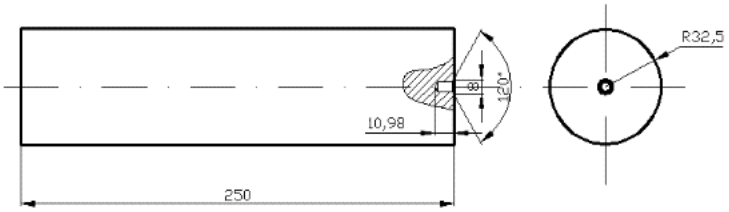

Fig. 4. AISI 1070 steel as the test material

2.4 Experimental equipment

1. Cutting tool

The cutting tool used in this study was a single-layer diamond-film-coated carbide insert with an ISO grade of N10, which is recommended for machining non-ferrous metals [18]. The insert geometry and dimensions conformed to ISO standards and were designated as DCGX 11T3 04-AL 1810. The technical specifications of the cutting tool are depicted in Fig. 5 and Table 5.

Type	Dimensions (mm)			
04-AL DCGX 11 T3	re	l	iC	S
	0.4	11	9.525	4
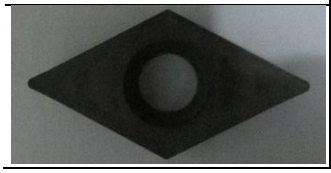	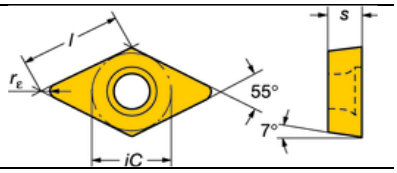			

Fig. 5. Cutting tool geometry: ISO Grade N10, DCGX 11T3 04-AL

2. Turning machine

The turning process was conducted using a CD 6260-C lathe. The technical specifications of the machine are depicted in Fig. 6.

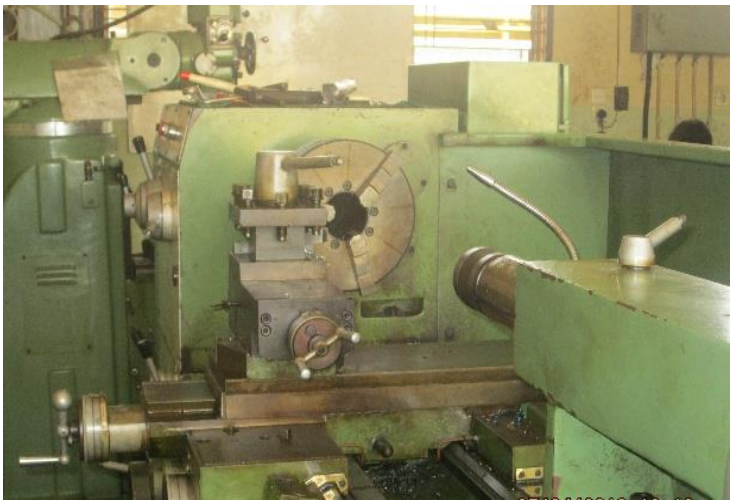

Fig. 6. CD 6260-C turning machine

Table 5. Properties and characteristics of carbide cutting tools (N10, DCGX 11T3 04-AL)

Composition						94% WC - 6% Co	
Coating thickness (µm)	Grain size (µm)	Hardness (HV)	Coating specification	Radius nose (mm)	Max Dept of cut (mm)	Max cutting speed (v=m/min)	Max feeding (mm)
6.0	1.4-2.5	1710	Diamond-film	0.4	1.5	2000	0.2

3. Portable hardness testing device

To measure the hardness value of the material, it was analyzed using a portable hardness tester, as depicted in Fig. 7.

Fig. 7. Portable hardness tester

4. USB digital microscope

Initial tool wear after machining was documented using a USB-based digital microscope imaging system. The system was equipped with dual-axis optical lenses providing magnifications of 27× (working distance 8 mm) and 100× (2 mm). The experimental setup of the USB digital microscope as depicted in Fig. 8.

Fig. 8. USB digital microscope

5. Scanning Electron Microscopy and Energy-Dispersive X-ray Spectroscopy (SEM–EDS analysis)

Microstructural and surface morphology analyses were conducted using Scanning Electron Microscopy (SEM) at a magnification of 20,000×. SEM is used to generate high-resolution images of surface topography and microstructural features through a focused electron beam, while elemental composition is analyzed using an integrated EDS system. The SEM-EDS instrument was used in this study as depicted in Fig. 9.

Fig. 9. Scanning electron microscopy with energy-dispersive X-ray spectroscopy

3 Results and discussion

The present study aims to identify the machining parameters that influence cutting performance and to characterize the applied tool coating. The investigation focuses on the effects of mechanical loads, thermal loads, and chemical interactions between the workpiece and the cutting tool, with particular emphasis on the diamond film coating and its substrate. Coating integrity was evaluated through delamination testing performed under dry machining conditions.

3.1 Research result

3.2 Research results on the effect of mechanical loading

The machining performance data for Al-6061 are presented in Table 6 and depicted in Figs. 10 and 11.

Table 6. Machining test results for Al-6061

No	v (m/min)	f (mm/rev)	a (mm)	d (mm)	n (rpm)	lt (mm)	t_c (min)	VB (mm)
1	385	0.15	1.5	145	845	55	0.43	0
2	385	0.15	1.5	145	845	110	0.87	0.035
3	385	0.15	1.5	145	845	165	1.30	0.051
4	385	0.15	1.5	145	845	220	1.74	0.164
5	385	0.15	1.5	145	845	275	2.17	0.194
6	385	0.15	1.5	145	845	330	2.60	0.224
7	385	0.15	1.5	145	845	385	3.04	0.239
8	385	0.15	1.5	145	845	440	3.47	0.254
9	385	0.15	1.5	145	845	495	3.91	0.269
10	385	0.15	1.5	145	845	550	4.34	0.284
11	385	0.15	1.5	145	845	605	4.77	0.313
12	385	0.15	1.5	145	845	660	5.21	0.42

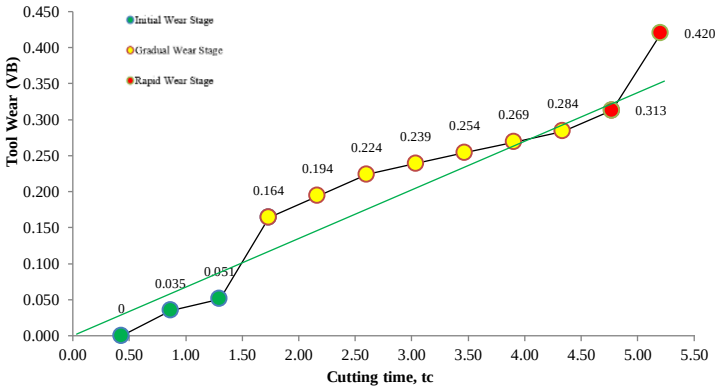

Fig. 10. Edge wear progression curve for Al-6061 at cutting speed 385 m/min, feed rate 0.15 mm/rev, cutting depth 1.5 mm

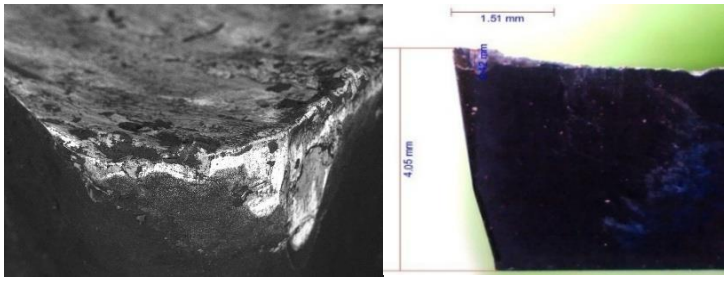

Fig. 11. Edge wear progression for Al-6061 (VB) 0.42 mm

The influence of mechanical loading on the machining performance of Al-6061 during the initial wear stage (tc) 1.74 min was evaluated under the machining conditions presented in Table 7 and Fig. 12. Machining test data for AISI 1070 material (Table 8, Figs. 13 and 14).

Table 7. Machining test results for Al-6061 during the initial wear stage

v (m/min)	f (mm/rev)	a (mm)	d (mm)	n (rpm)	lt (mm)	t_c (min)	t_c (s)	VB (mm)	VB° (mm/s)
385	0.15	1.5	145	845	220	1.74	104.4	0.07	0.0007

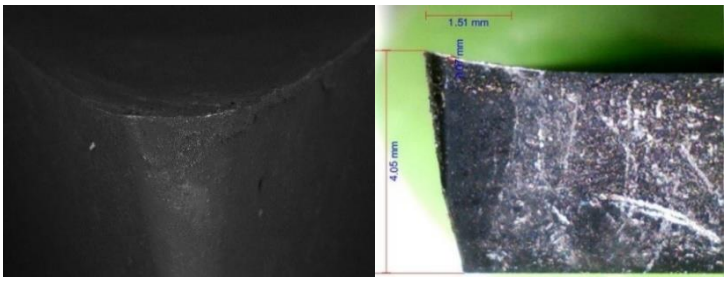

Fig. 12. Abrasive wear during the initial wear stage of the diamond film-coated carbide tool in machining Al-6061, cutting speed 385 m/min; tc 1.74 min; VB 0.07 mm

Table 8. Machining test results for AISI 1070

No	v (m/min)	f (mm/rev)	a (mm)	d (mm)	n (rpm)	lt (mm)	t_c (min)	VB (mm)
1	111	0.15	1.5	65	545	30	0.37	0
2	111	0.15	1.5	65	545	30	0.73	0.06
3	111	0.15	1.5	65	545	60	1.1	0.16
4	111	0.15	1.5	65	545	90	1.47	0.22
5	111	0.15	1.5	65	545	120	1.83	0.24
6	111	0.15	1.5	65	545	150	2.20	0.27
7	111	0.15	1.5	65	545	180	2.57	0.28
8	111	0.15	1.5	65	545	210	2.94	0.39

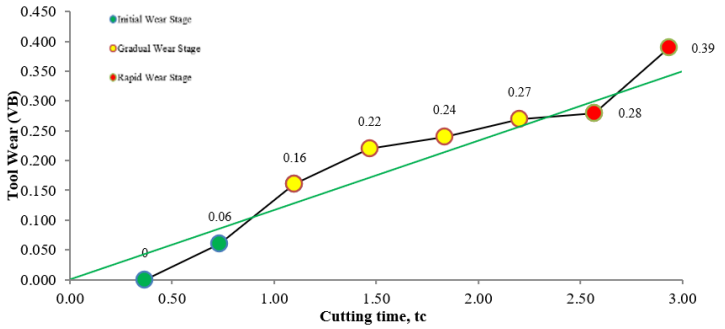

Fig. 13. Edge wear progression curve for AISI 1070 at cutting speed 111 m/min; feed rate 0.15 mm/rev; cutting depth 1.5 mm

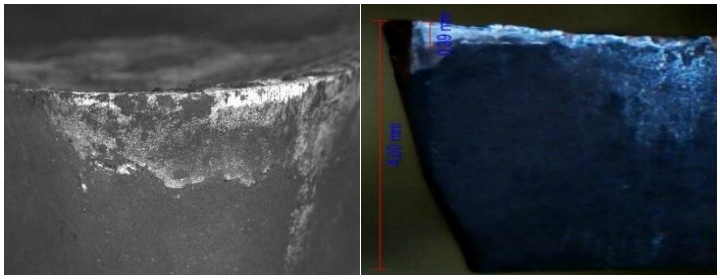

Fig. 14. Edge wear progression of AISI 1070 (VB) 0.39 mm

An investigation was conducted to evaluate the influence of mechanical loading on the machining performance of AISI 1070 during the initial wear stage (tc) 1.1 min. The experiments were performed under the machining parameters presented in Table 9 and Fig. 15.

Table 9. Machining test results of AISI 1070 during the initial wear stage

v (m/min)	f (mm/rev)	a (mm)	d (mm)	n (rpm)	lt (mm)	t_c (min)	t_c (s)	VB (mm)	VB° (mm/s)
111	0.15	1.5	65	545	60	1.1	66	0.25	0.0038

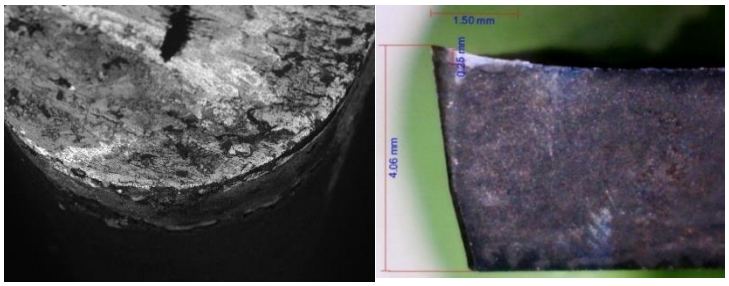

Fig. 15. Flank wear (VB) 0.25 mm observed during the initial wear stage of the coated carbide tool in the machining of AISI 1070

3.2.1 Research results on the effect of thermal loading

The performance of the diamond film-coated carbide tool during the initial wear stage in the machining of Al-6061 is summarized in Table 10 and presented in Fig. 16.

Table 10. Results of thermal loading tests on Al-6061 at a 20% increase in cutting speed

v (m/min)	f (mm/rev)	a (mm)	d (mm)	n (rpm)	lt (mm)	t_c (min)	t_c (s)	VB (mm)	VB° (mm/s)
462	0.15	1.5	128	1150	300	1.74	104.4	0.1	0.0009

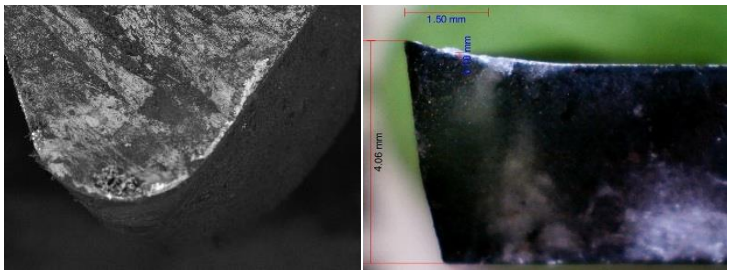

Fig. 16. Edge wear observed during the initial wear stage of the coated carbide tool of Al-6061

The performance of the diamond film-coated carbide tool during the initial wear stage in the machining of AISI 1070 is summarized in Table 11 and presented in Fig. 17.

Table 11. Results of thermal loading tests on AISI 1070 at a 20% reduction in cutting speed

v (m/min)	f (mm/rev)	a (mm)	d (mm)	n (rpm)	lt (mm)	t_c (min)	t_c (s)	VB (mm)	VB° (mm/s)
89	0.15	1.5	52	545	60	1.1	66	0.16	0.0024

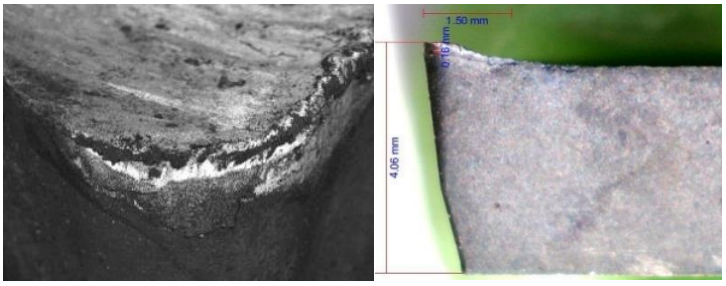

Fig. 17. Flank wear (VB) 0.16 mm and plastic deformation observed during the initial wear stage of the coated carbide tool of AISI 1070

3.2.2 Research results on the effect of chemical interactions

Analysis of the diamond film coating on the cutting tool was carried out during Al-6061 machining at a cutting speed of 385 m/min within the initial wear stage (tc 1.74 min; VB 0.07 mm). The obtained results are summarized in Table 12 and presented in Figs. 18 and 19.

Table 12. EDS analysis of the diamond film coating for machining of Al-6061 at a cutting speed of 385 m/min

Element	Weight%	Atomic%	Information
		Spectrum^{-1}	
Carbon	99.113	99.854	Significant diamond film elements
Tungsten	0.260	0.017	
Cobalt	0.626	0.129	
		Spectrum^{-2}	
Carbon	99.947	99.997	Significant diamond film elements
Tungsten	0.260	0.003	

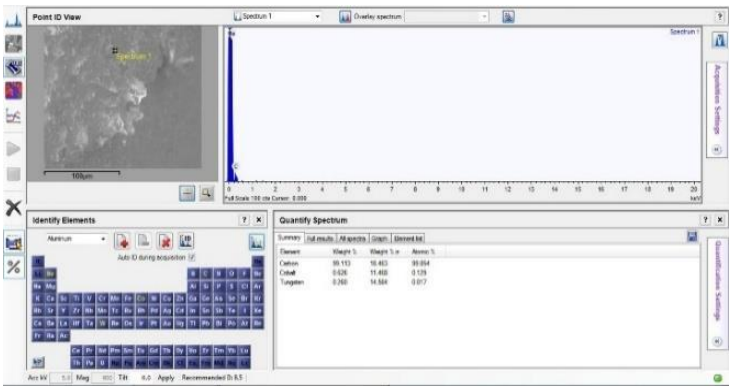

Fig. 18. EDS elemental spectrum [1] of the diamond film coating during the machining of Al-6061 at a cutting speed of 385 m/min

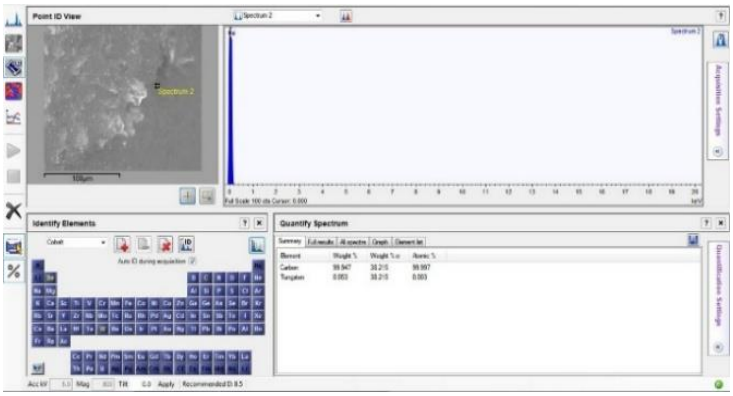

Fig. 19. EDS elemental spectrum [2] of the diamond film coating during machining of Al-6061 at a cutting speed of 385 m/min

Subsequently, machining tests were conducted at a cutting speed of 462 m/min. During the initial wear stage (tc) 1.74 min, the measured flank wear (VB) was 0.1 mm in the machining of Al-6061. The corresponding results are presented in Table 13 and illustrated in Figs. 20 and 21.

Table 13. Elemental of the diamond film coating at a cutting speed of 462 m/min during the machining of Al-6061

Element	Weight%	Atomic%	Information
		Spectrum^{-1}	
Carbon	85.124	94.329	Significant diamond film elements
Magnesium	0.239	0.131	
Aluminum	9.770	4.819	
Silicon	0.775	0.367	
Cobalt	0.369	0.083	
Tungsten	3.722	0.269	
		Spectrum^{-2}	
Carbon	99.968	99.992	Significant diamond film elements
Magnesium	0.003	0.002	
Aluminum	0.004	0.002	
Silicon	0.007	0.003	
Copper	0.004	0.001	
Tungsten	0.015	0.001	

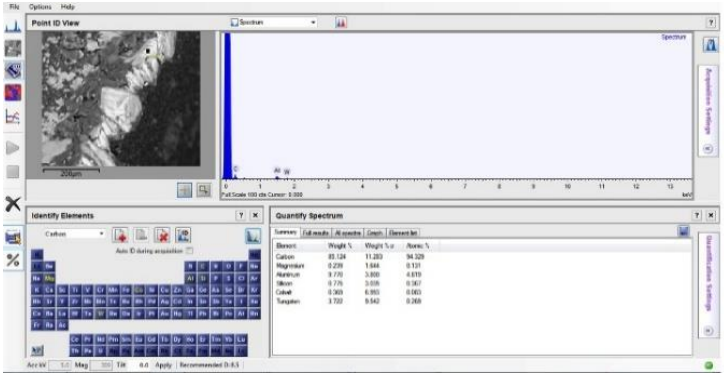

Fig. 20. EDS elemental spectrum [1] obtained during the machining of Al-6061 under the cutting speed 462 m/min

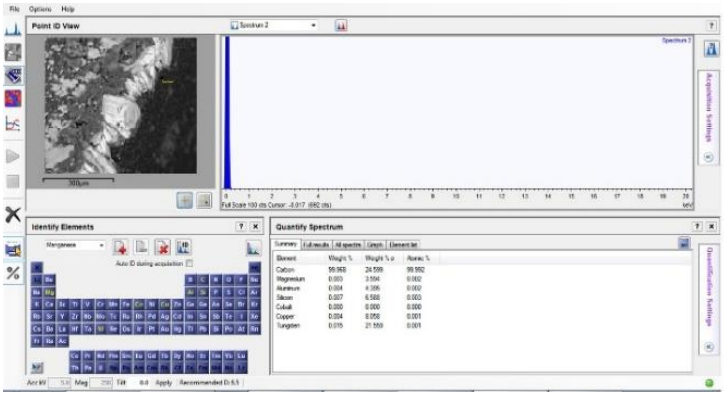

Fig. 21. EDS elemental spectrum [2] obtained during the machining of Al-6061 under the cutting speed of 462 m/min

Analysis of the diamond film layer on the cutting tool was conducted during the machining of AISI 1070 at a cutting speed of 111 m/min. During the initial wear stage (tc) 1.1 min, the measured flank wear reached (VB) 0.25 mm. The experimental data are summarized in Table 14 and presented in Figs. 22 and 23.

Table 14. Elemental composition of the diamond film coating at a cutting speed of 111 m/min during the machining of AISI 1070

Element	Weight%	Atomic%	Information
		Spectrum-1	
Carbon	34.623	67.573	The coating element (diamond-film) is not significant
Chromium	44.181	19.918	
Cobalt	8.130	3.234	
Fluorine	6.878	6.878	
Tungsten	6.189	0.789	
		Spectrum-2	
Carbon	79.547	95.698	Significant diamond-film coating elements
Tungsten	4.277	0.336	
Cobalt	16.175	3.966	

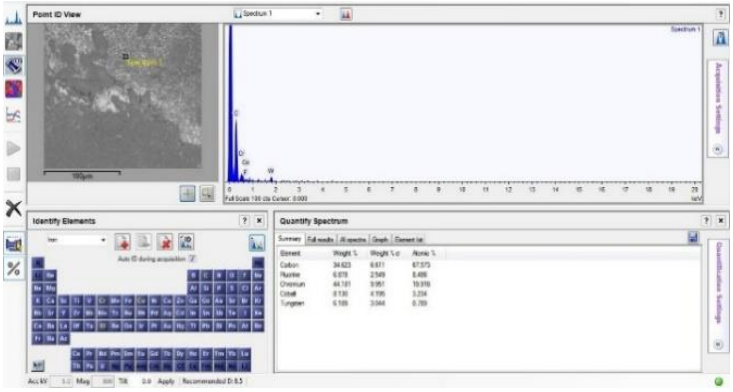

Fig. 22. EDS elemental spectrum [1] obtained during the machining of AISI 1070 at a cutting speed of 111 m/min

The diamond film coating on the carbide tool was further analyzed during the machining of AISI 1070 at a cutting speed of 89 m/min. During the initial wear stage (TC) 1.1 min, the measured flank wear (VB) was 0.16 mm. The results are summarized in Table 15 and presented in Figs. 24 and 25.

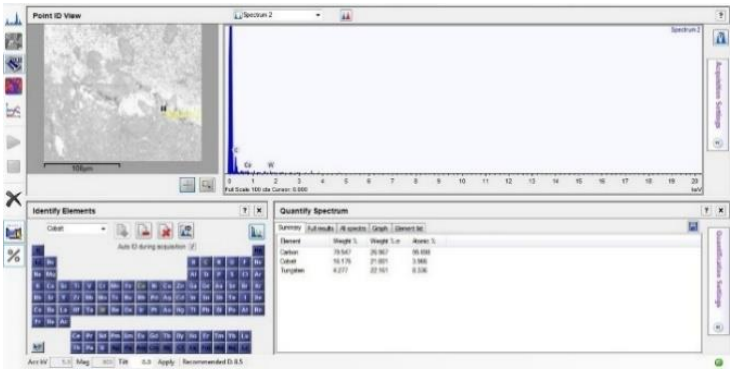

Fig. 23. EDS elemental spectrum [2] obtained during the machining of AISI 1070 at a cutting speed of 111 m/min

Table 15. Elemental composition of the diamond film coating at a cutting speed of 89 m/min during the machining of AISI 1070

Element	Weight%	Atomic%	Information
		Spectrum-1	
Carbon	12.253	35.105	The coating element (diamond film) is not significant
Fluorine	4.398	7.967	
Aluminum	0.113	0.144	
Silicon	0.384	0.470	
Titanium	37.093	26.648	
Chromium	39.073	25.860	
Iron	2.389	1.472	
Cobalt	3.759	2.195	
Zinc	0.111	0.059	
Tungsten	0.427	0.080	
		Spectrum-2	
Carbon	99.954	99.997	Significant diamond film elements
Tungsten	0.046	0.003	

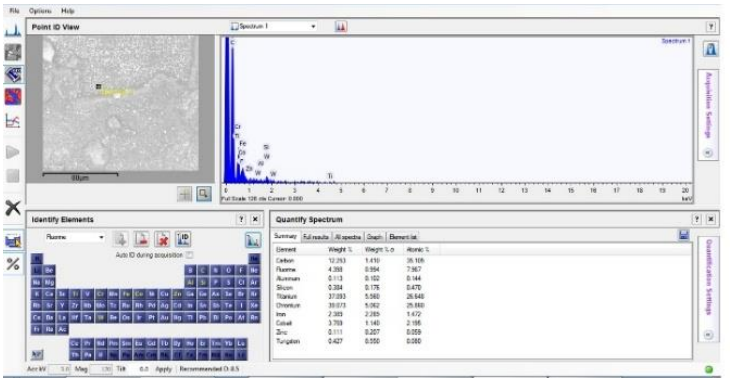

Fig. 24. EDS elemental spectrum [1] was obtained at cutting speed 89 m/min, AISI 1070 (tc) 1.1 min, with a measured flank wear (VB) 0.16 mm

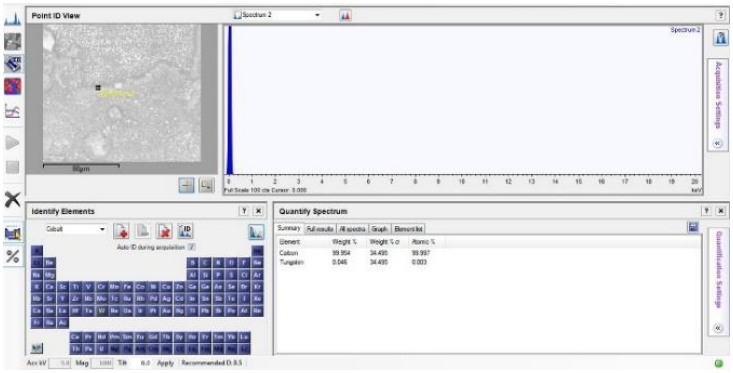

Fig. 25. EDS elemental spectrum [2] was obtained at cutting speed 89 m/min, AISI 1070 (tc) 1.1 min, with a measured flank wear (VB) 0.16 mm

3.3 Discussion

3.3.1 Effect of mechanical loading

The results presented in Table 7 and Fig. 12 demonstrate distinct wear characteristics under different mechanical loading conditions. During the machining of Al-6061, flank wear developed gradually within the initial wear stage (tc) 1.74 min, reaching (VB) 0.07 mm with an average wear rate (VB°) 0.0007 mm/s. Localized abrasive wear at the cutting edge was identified as the primary flank wear mechanism. Since the measured flank wear remained well below the allowable limit (VB_{max} 0.3 mm), the tool did not reach the failure criterion. These findings indicate that the moderate mechanical loading encountered during the machining of this non-ferrous alloy did not cause significant degradation of the diamond film coating or damage to the WC/Co substrate. The present results suggest that the coating material functions as a solid lubricant, thereby suppressing frictional interaction and reducing thermal loading, which are critical factors in improving cutting performance and mitigating tool wear [3]. This behavior aligns with established tribological theories in metal cutting [15].

In contrast, the results presented in Table 9 and Fig. 15 indicate that the machining of AISI 1070 under higher mechanical loading conditions significantly accelerated flank wear, resulting in a (VB) 0.25 mm and a wear rate (VB°) 0.0038 mm/s after a cutting time (tc) of 1.1 min. The combined effects of the higher workpiece hardness, increased feed rate, and greater depth of cut intensified the contact stresses at the tool-workpiece interface. These conditions promoted rapid material removal at the tooltip, causing progressive changes in tool geometry and reducing contact stability during machining. The results demonstrate that mechanical loading plays a dominant role in accelerating wear progression and initiating tool degradation. Consequently, continued wear development is expected to diminish the effectiveness of tool-workpiece contact during prolonged cutting operations. Consistent with previous findings [4], cutting conditions have been identified as critical factors influencing the wear behavior and tool life of coated carbide tools. Therefore, appropriate selection and optimization of machining parameters are essential for achieving optimal machining performance.

3.3.2 Effect of thermal loading

The results presented in Table 10 indicate that a 20% increase in cutting speed during the machining of Al-6061 had only a limited effect on flank wear progression. At a cutting speed of 462 m/min, flank wear (VB) of 0.10 mm with a wear rate (VB°) of 0.0009 mm/s, remained within the initial wear stage (tc) 1.74 min. The wear pattern was distributed uniformly along the tool-workpiece contact zone, indicating stable thermal conditions throughout the machining process. The relatively low hardness of the workpiece material reduced the severity of contact stresses acting on the cutting tool, thereby limiting wear development. Consequently, the increase in cutting speed mainly influenced the tool-workpiece contact interaction without inducing significant thermal degradation or accelerated wear. As illustrated in Fig. 16, the uniform distribution of longitudinal flank wear along the contact zone further confirms the excellent thermal stability and wear resistance of the diamond film coated carbide tool under the investigated cutting condition. The findings of the present study are inconsistent with those reported by [10], who identified increasing cutting speed as the primary factor promoting coating failure in coated carbide tools.

In contrast, the results presented in Table 11 show that the machining of AISI 1070 at a 20% lower cutting speed of 89 m/min resulted in more pronounced wear progression, with flank wear (VB) 0.16 mm and a wear rate (VB°) 0.0024 mm/s. Wear propagation toward the cutting-edge angle was accompanied by localized plastic deformation, as illustrated in Fig. 17. Furthermore, the formation of adhered material layers in the form of a BUE was observed during the initial wear stage (tc) 1.1 min. Although the cutting speed was relatively low, the larger depth of cut applied under the cutting speed variation condition increased thermal loading during machining. This condition intensified contact pressure and adhesion forces at the tool-workpiece interface, thereby accelerating flank wear and promoting localized plastic deformation. These results suggest that thermal effects become increasingly important when combined with high cutting forces generated during the machining of harder workpiece materials. The analysis of machining parameter variations at reduced cutting speeds indicated that the critical fatigue strain decreased markedly with increasing strain rate, leading to a significant reduction in tool life. This behavior can be attributed to the limited time available for dislocation motion within the material at higher strain rates, which promotes the formation of localized stress concentration zones [9].

3.3.3 Effect of chemical interactions

Chemical interaction analysis using EDS was conducted to evaluate coating integrity and potential interfacial degradation. During the machining of Al-6061 at a cutting speed of 385 m/min, the EDS results presented in Table 12 showed carbon concentrations exceeding 99% in both spectrum [1] and spectrum [2]. These values indicate that the diamond film coating remained intact throughout the analyzed regions. In the area subjected to abrasive wear, the coating effectively protected the WC/Co substrate and showed no evidence of degradation or chemical modification from external factors. At a 20% increase in cutting speed to 462 m/min, the results presented in Table 13 showed carbon concentrations exceeding 94% in both spectrum [1] and spectrum [2], confirming that no coating delamination occurred. Further elemental analysis detected the presence of aluminium, magnesium, and silicon, in addition to carbon and the constituent elements of the WC/Co substrate. These elements originated from the workpiece material and were likely diffused into the coating region as a result of the increased cutting speed accompanied by a rise in cutting temperature. Nevertheless, the high carbon content detected in both spectra indicates that the diamond film coating maintained good chemical stability and experienced only minimal chemical degradation throughout the machining process. Furthermore, the analyzed regions exhibited a fully preserved coating structure with no evidence of interfacial failure under the investigated cutting-speed conditions. The absence of coating delamination indicates that the diamond film-coated carbide tool maintained its structural integrity throughout the entire range of cutting speeds evaluated in this study. This behavior differs from the findings reported in [10], which identified increasing cutting speed as a primary factor promoting coating failure in coated carbide tools. This discrepancy suggests that the susceptibility of a coating to delamination under high cutting speed conditions is strongly influenced by the characteristics of the coating, the properties of the workpiece material, and the machining conditions employed.

The machining of AISI 1070 resulted in localized elemental redistribution within the analyzed wear region. As presented in Table 14, at a cutting speed of 111 m/min, the carbon concentration, which represents the principal constituent of the diamond film coating, decreased to 67.573% in spectrum [1]. This reduction was accompanied by the detection of Cr, Co, and W, indicating localized thinning of the coating layer and partial exposure of the underlying tool substrate. The presence of these elements, originating from both the WC/Co substrate and the workpiece material, suggests the occurrence of material transfer and diffusion within the tool-workpiece contact zone. The reduction in carbon concentration, together with the appearance of foreign elements, confirms that progressive abrasive wear had degraded the diamond film coating in this region. This localized degradation is consistent with the high mechanical loading experienced during the initial wear stage (tc) 1.1 min, where elevated contact stresses promoted coating damage within the critical tool-workpiece interface. Although the diamond film coating possesses exceptional hardness, its inherent brittleness may increase its susceptibility to localized fracture and subsequent abrasive removal under severe loading conditions. In contrast, spectrum [2] exhibited a carbon concentration of 95.698%, indicating that the coating remained largely intact in this region. This observation suggests that coating degradation was not uniformly distributed across the tool surface but was concentrated in localized high-stress contact areas, while other regions maintained good coating integrity. The results further suggest that excessive contact pressure may inhibit the formation of protective deposits at the cutting edge, whereas appropriate contact conditions are required to promote the development of stable protective layers during turning operations. Therefore, optimization of tool-workpiece contact conditions is essential for enhancing the protective capability and wear resistance of diamond film-coated carbide tools during the machining of AISI 1070. The present results corroborate the findings reported by [8], indicating that mechanical fracture is the dominant wear mechanism controlling tool degradation. Moreover, carbon diffusion from the WC substrate and the Co binder contributed significantly to the acceleration of wear progression during the machining of Ti6Al4V titanium alloy.

Under the reduced cutting speed condition of 89 m/min, the EDS results presented in Table 15 revealed a carbon concentration of

35.105% in spectrum [1], indicating substantial degradation of the diamond film coating due to severe abrasive wear. The significant reduction in carbon content confirms extensive removal of the coating layer and localized exposure of the underlying tool substrate within the analyzed region. This coating degradation is primarily associated with mechanical wear mechanisms, particularly the combined effects of cutting pressure and cutting forces that exceeded the adhesive strength of the coating during machining. In addition to abrasive wear, localized plastic deformation was observed along the tool edge. This deformation is attributed to the high contact pressure generated by the hardness of the workpiece material, together with the thermal conditions associated with the reduced cutting speed. As a consequence, dimensional irregularities developed at the cutting-edge angle, leading to progressive changes in tool geometry. Furthermore, the wear process facilitated the formation of a BUE, which was observed adhering to the cutting-edge region. The wear evolution was characterized by an initial stage of relatively low wear, followed by a rapid increase in flank wear as abrasive damage intensified. These findings suggest that prolonged machining under such conditions may significantly increase the risk of tool failure or fracture due to the combined effects of severe abrasive wear, plastic deformation, and BUE formation. Consistent with the findings reported in [8], oxidation of the Co binder was identified as a contributing factor to the degradation of the mechanical integrity of TiAlN–NbN-coated carbide tools during the machining of Ti6Al4V titanium alloy. Moreover, the combined effects of elemental diffusion and binder oxidation significantly accelerated the progression of tool wear.

Conversely, the EDS results presented in Table 15 for spectrum [2] revealed a carbon concentration of 99.997%, indicating that the diamond film coating remained intact in this region. This observation suggests that, despite the occurrence of localized coating degradation under reduced cutting speed conditions, other critical areas of the tool surface retained a stable diamond film layer capable of effectively protecting the WC/Co substrate. The localized abrasive degradation of the coating is closely related to the prevailing mechanical loading conditions. Elevated contact pressure and cutting forces are presumed to have exceeded the coating adhesion strength, thereby promoting coating damage during the initial wear stage (tc) 1.1 min. The reduction in carbon concentration observed in the affected regions is therefore indicative of abrasive wear accompanied by localized coating removal.

Overall, the results indicate that the observed coating degradation was predominantly driven by mechanically induced stresses, especially the elevated contact pressure and cutting forces generated at the tool-workpiece interface. These findings suggest that both mechanical loading and chemical interactions play dominant roles in controlling abrasive wear and localized degradation of the diamond film coating within the critical contact region. Therefore, identifying an appropriate range of machining parameters is essential for achieving optimal cutting performance. This observation is consistent with the findings reported by [13], who demonstrated that excessively high contact pressure suppresses the formation of protective deposits at the tool edge, whereas excessively low contact pressure accelerates excessive wear on the surface of PVD (Ti,Al)N-coated carbide tools during the turning of 316L stainless steel. Furthermore, investigations into tool wear are crucial for understanding the influence of machining parameters on coating delamination. As reported by [14], nano-diamond-coated cutting tools were evaluated during the machining of aluminum matrix composites, where wear behavior was consistently observed under all machining conditions investigated. The authors further identified the feed rate as the dominant machining parameter governing the cutting duration before coating delamination, primarily because of the increased mechanical loading imposed on the cutting tool. Similar observations were reported in the experimental investigation of ASTM A29 steel machining using TiAlN-coated carbide tools, which demonstrated that satisfactory cutting performance can be achieved only within an appropriate range of machining parameters and operating conditions [6].

4 Conclusions

Effects of machining parameters on cutting performance and coating wear mechanisms of coated carbide tools were systematically evaluated through experimental investigation and comprehensive analytical observations. The principal findings of the study are summarized as follows:

1. Mechanical loading was the dominant factor affecting tool wear. During Al-6061 machining, abrasive wear was limited, with flank wear (VB) of 0.07 mm. In AISI 1070 machining, higher mechanical loading accelerated wear development to a VB of 0.25 mm and increased tool degradation.
2. Thermal loading had limited influence during Al-6061 machining. However, in AISI 1070 machining, thermal effects combined with high contact pressure promoted faster wear progression, plastic deformation, and BUE formation.
3. The diamond film coating maintained chemical stability during Al-6061 machining, with no delamination observed. In AISI 1070 machining, localized abrasive wear caused partial coating loss and substrate exposure, indicating progressive degradation rather than coating failure.
4. Abrasive wear was the dominant wear mechanism, while thermally activated degradation and chemical interactions had smaller contributions. The brittleness of the diamond film increased its susceptibility to localized wear under harder ferrous machining conditions. These findings provide a basis for improving coated cutting tool performance and support future studies on cutting temperature, adhesion behavior, and coating fatigue resistance.

References

[1] Vitor F. C. Sousa, Francisco José Gomes Da Silva, Gustavo Filipe Pinto, Andresa Baptista and Ricardo Alexandre. Characteristics and Wear Mechanisms of TiAlN-Based Coatings for Machining Applications, Metals, 11(2), 260, pp 1-49, 2021, https://doi.org/10.3390/met11020260.

[2] Harshit B. Kulkarni a, Mahantesh M. Nadakatti a, Sachin C. Kulkarni a, Raviraj M. Kulkarni. Investigations on effect of nanofluid based minimum quantity lubrication technique for surface milling of Al7075-T6 aerospace alloy, Materials Today, vol 27(1), pp 251-256, 2020, https://doi.org/10.1016/j.matpr.2019.10.127.

[3] M. Nouari, A. Ginting. Wear characteristics and performance of multi-layer CVD-coated alloyed carbide tool in dry end milling of titanium alloy, Surface and Coatings Technology, vol 200, issues 18-19, pp 5663-5676, 2006. https://doi.org/10.1016/j.surfcoat.2005.07.063.

[4] Yanuar Burhanuddin, Suryadiwansa Harun, Gusri A. Ibrahim, Arinal Hamni. Optimization of tool wear and surface roughness in ST-37 steel turning process with varying tool angles and machining parameters, Jurnal Polimesin, vol 22, no. 3, pp 315-318, 2024, http://dx.doi.org/10.30811/jpl.v22i3.4983.

[5] Arfan Halim, Ilmawan Suryapradana, Dedy S, Experimental investigation of tool wear TiAlN(Al2O3)/TiN-coated carbide in the cam-shaft turning process, Jurnal Polimesin, vol 20, no. 2, pp 155-161, 2022, http://dx.doi.org/10.30811/jpl.v20i2.2962.

[6] Rizki Ramadhan, Sunarto Sunarto. Studi eksperimental pertumbuhan aus sisi (vb) pahat karbida berlapis Titanium Aluminium Nitrida (TiAlN) pada pembubutan basah baja ASTM A29, vol 17, no. 2, pp 75-82, 2019, http://dx.doi.org/10.30811/jp.v17i2.1020.

[7] C.H. Che Haron, A. Ginting, H. Arshad. Performance of alloyed uncoated and CVD-coated carbide tools in dry milling of

titanium alloy Ti-6242S, Journal of Materials Processing Technology, vol 185, issues 1-3, pp 77-83, 2007, https://doi.org/10.1016/j.jmatprotec.2006.03.135.

[8] Rebecka Lindvall, Josu Casas Gayubo, Oleksandr Gutnichenko, François Auzenat, Rachid M'Saoubi, Volodymyr Bushlya. Performance and wear mechanisms of TiAlN-NbN coated cemented carbide n milling Ti6Al4V with different cooling and lubrication approaches, International Journal on the Science and Technology of Wear, vol 571, pp 1-9, 2025, https://doi.org/10.1016/j.wear.2025.205846.

[9] Antonios Bouzakis, Georgios Skordaris, Emmanouil Bouzakis, Konstantinos-Dionysios Bouzakis, and Dimitrios Tsakalidis. Wear Evolution on PVD Coated Cutting Tool Flank and Rake Explained Considering Stress, Strain and Strain-Rate Dependent Material Properties, Coatings, vol 13, issues 12, pp 1-17, 2023, https://doi.org/10.3390/coatings13121982.

[10] J. Hu a, Y.K. Chou a,*, R.G. Thompson. Nanocrystalline diamond coating tools for machining high-strength Al alloys, International Journal of Refractory Metals and Hard Materials, vol 26, issues 3, pp 135-144, 2008, https://doi.org/10.1016/j.ijrmhm.2007.05.012.

[11] Axel Bjerke, Andrii Hrechuk, Filip Lenrick, Rachid M'Saoubi, Henrik Larsson, Andreas Markstrom, Thomas Bjork, Susanne Norgren, Jan-Eric Ståhl, Volodymyr Bushlya. Onset of the degradation of CVD α-Al2O3 coating during turning of Ca-treated steels, International Conference on Wear of Materials, vol 447, pp 1-10, 2021 https://doi.org/10.1016/j.wear.2021.203785.

[12] A. Bjerke et al. Understanding wear and interaction between CVD α-Al2O3 coated tools, steel, and non-metallic inclusions in machining, Surface & Coatings Technology, vol 450, pp 1-11, 2022, https://doi.org/10.1016/j.surfcoat.2022.128997.

[13] Axel Bjerke, Filip Lenrick, Andrii Hrechuk, Kateryna Slipchenko, Rachid M'Saoubi, Jon M. Andersson, Volodymyr Bushlya. On chemical interactions between an inclusion engineered stainless steel (316L) and (Ti,Al)N coated tools during turning, Wear, vol 532-533, pp 1-12, 2023, https://doi.org/10.1016/j.wear.2023.205093.

[14] F. Qin, J. Hu, Y.K. Chou, R.G. Thompson. Delamination wear of nano-diamond coated cutting tools in composite machining, Wear, vol 267, issues 5-8, pp 991-995, 2009, https://doi.org/10.1016/j.wear.2008.12.065.

[15] Serope Kalpakjian and Steven R. Schmid,"Manufacturing Processes for Engineering Materials", ixth Edition in SI Units, K. S. Vijay Sekar, Pearson Education Limited, United Kingdom, 2023.

[16] T. Rochim, Perkakas dan Sistem Pemerkakasan Umur Pahat, Cairan Pendingin. Bandung: ITB, 2007.

[17] Material Property Data, Materials Information, 2025, https://www.matweb.com/.

[18] Sandvik Coromant, General Catalogue, 2025, https://www.sandvik.coromant.com/en-gb/tools/turning-tools.